

Images in Cardiovascular Medicine



Customized Fenestrated Thoracic Endovascular Aneurysm Repair in an Elderly Patient With Complex Visceral Anatomy

Jun-Chang Jeong , MD, Jaeoh Lee , MD, Sun-Oh Kim , MD, and Young-Guk Ko , MD, PhD

Division of Cardiology, Severance Cardiovascular Hospital, Yonsei University Health System, Seoul, Korea

OPEN ACCESS

Received: Jun 5, 2025

Revised: Jul 25, 2025

Accepted: Aug 27, 2025

Published online: Oct 1, 2025

Correspondence to

Young-Guk Ko, MD, PhD

Division of Cardiology, Severance Cardiovascular Hospital, Yonsei University Health System, 50-1, Yonsei-ro, Seodaemun-gu, Seoul 03722, Korea.
Email: ygko@yuhs.ac

Copyright © 2025. The Korean Society of Cardiology

This is an Open Access article distributed under the terms of the Creative Commons Attribution Non-Commercial License (<https://creativecommons.org/licenses/by-nc/4.0>) which permits unrestricted noncommercial use, distribution, and reproduction in any medium, provided the original work is properly cited.

ORCID iDs

Jun-Chang Jeong

<https://orcid.org/0009-0002-6778-6151>

Jaeoh Lee

<https://orcid.org/0009-0002-5208-0498>

Sun-Oh Kim

<https://orcid.org/0000-0003-2851-7813>

Young-Guk Ko

<https://orcid.org/0000-0001-7748-5788>

Funding

The authors received no financial support for the research, authorship, and/or publication of this article.

An 88-year-old male with chronic kidney disease and hypertension was admitted for thoracic endovascular aneurysm repair (TEVAR) due to a rapidly enlarging thoracoabdominal aortic aneurysm involving the superior mesenteric artery (SMA) and abutting both renal arteries. The aneurysm measured 74 mm in diameter, and the celiac trunk was occluded at its origin (**Figure 1**). Given the patient's age and comorbidities, open surgery was high-risk, and the anatomy unsuitable for standard TEVAR. After shared decision-making, a customized fenestrated TEVAR (f-TEVAR) was selected.

Based on computed tomography (CT) analysis, a patient-specific fenestrated stent graft (SEAL 30-26×130 mm; S&G Biotech, Yongin, Korea) was designed with fenestrations aligned to the visceral artery origins (**Figure 2**). Pre-procedural aortography confirmed visceral artery involvement (**Figure 3A**).

Under local anesthesia, the fenestrated stent graft was deployed via the right femoral artery (**Figure 3B**), followed by bridging grafts to the right renal artery (BeGraft 6×38 mm; Bentley InnoMed, Hechingen, Germany) flared with a Mustang 7×40 mm balloon (Boston Scientific, Marlborough, MA, USA), to the SMA (BeGraft 9×37 mm) via the left brachial artery (**Figure 3C**), and to the left renal artery (Lifestream 7×37 mm, BD, Franklin Lakes, NJ, USA), also flared via the right femoral approach (**Figure 3D**). Additional proximal grafts (SEAL 34×80 mm and 42-36×130 mm) ensured sealing. Post-procedural aortography confirmed accurate positioning and branch patency (**Figure 3E and F**).

A one-week follow-up CT scan demonstrated aneurysm exclusion without endoleak and preserved bridging stent patency (**Figure 4**). A left brachial artery pseudoaneurysm was repaired surgically. No spinal cord ischemia occurred.

Customized f-TEVAR is a viable option for high-risk patients with complex anatomy.¹⁻⁴⁾ Informed consent was obtained from the patient for publication.

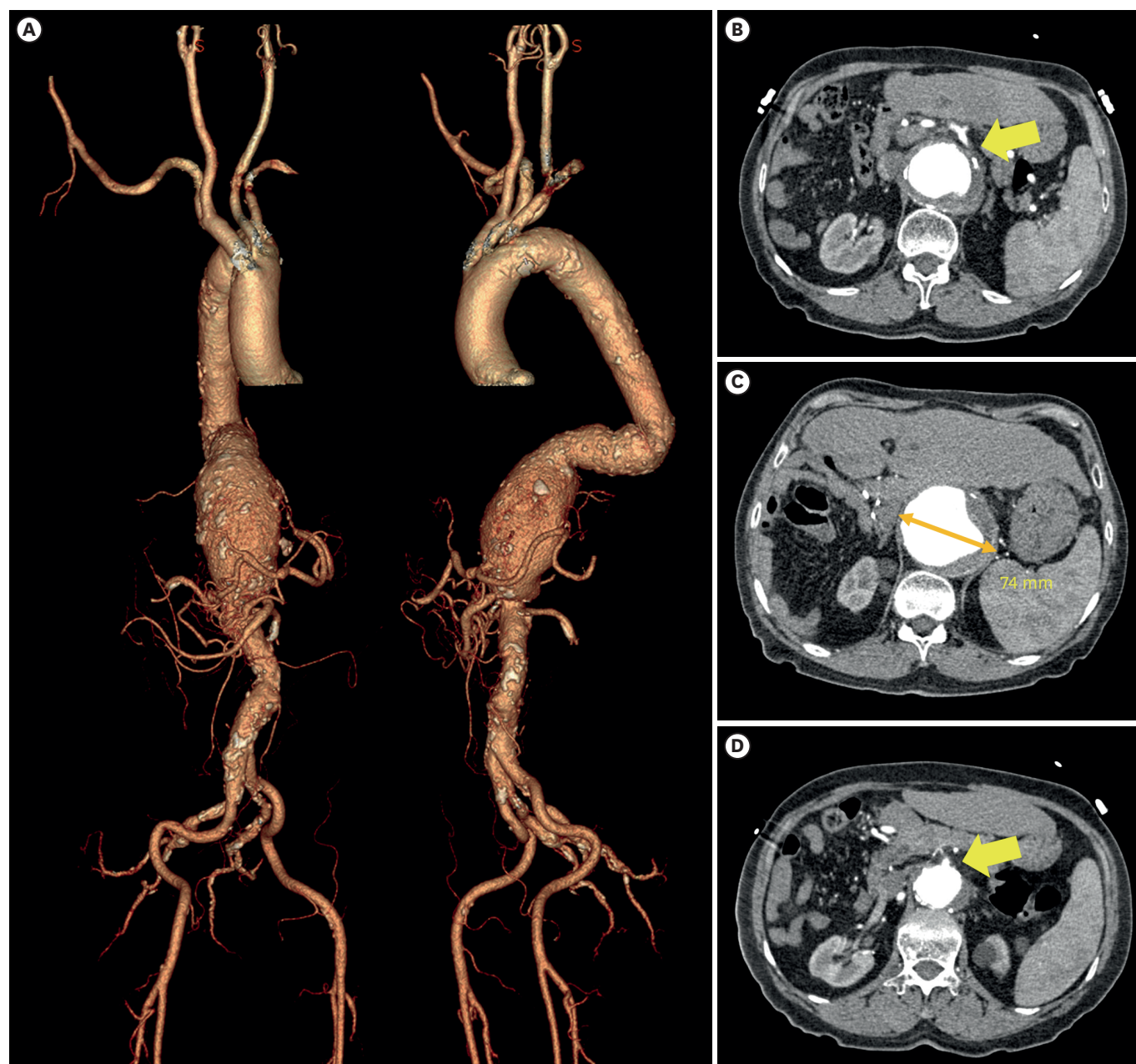


Figure 1. Pre-procedural computed tomography. (A) Volume-rendered 3-dimensional reconstruction image showing a tortuous thoracoabdominal aortic aneurysm with involvement of the visceral arteries. (B) Axial CT image demonstrating occlusion at the ostium of the celiac trunk (arrow). (C) Axial CT image showing the maximum aneurysm diameter of 74 mm. (D) Axial CT image of the distal aneurysmal segment involving the origin of the superior mesenteric artery (arrow). CT = computed tomography.

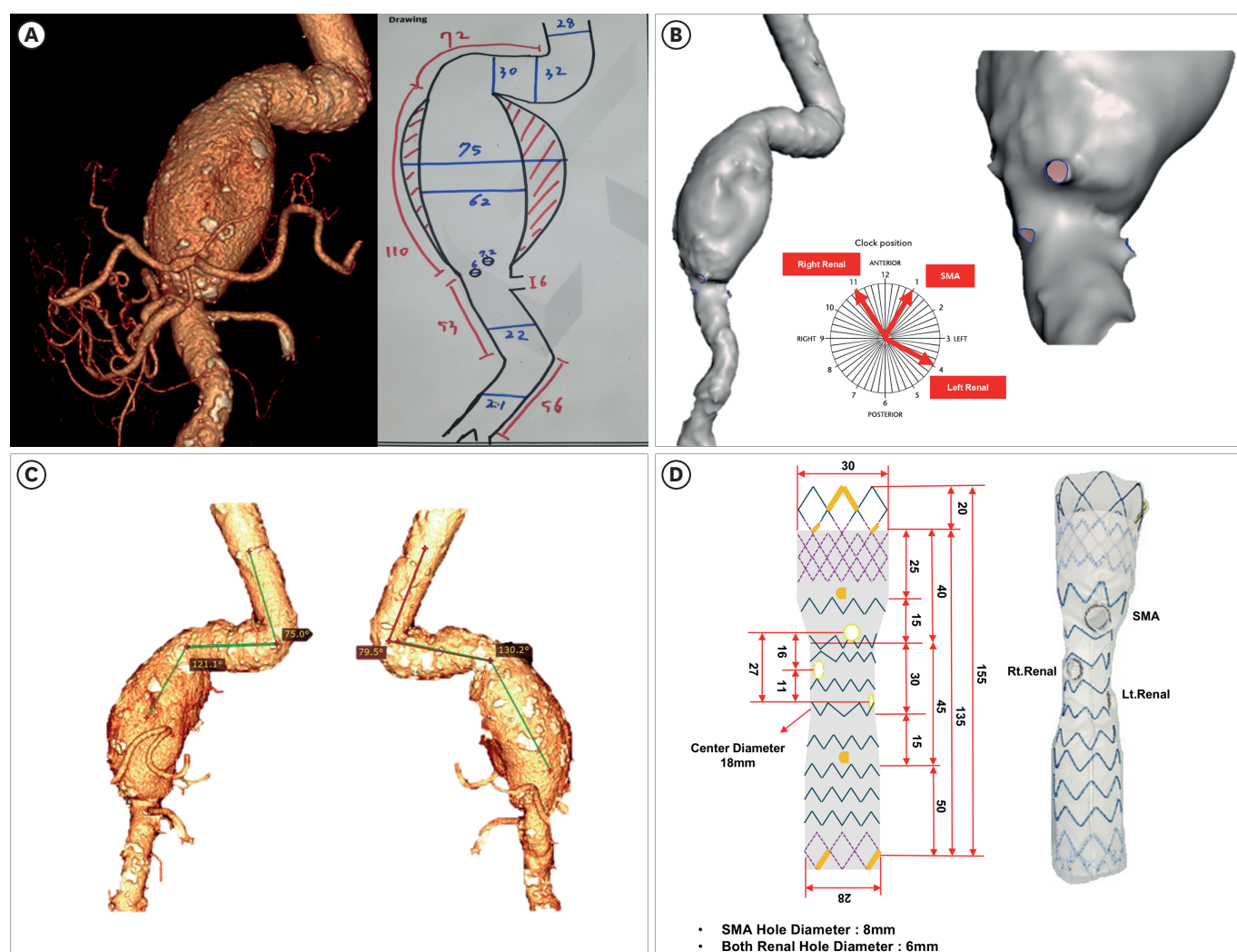


Figure 2. Pre-procedural planning and graft customization. (A) Volume-rendered 3-dimensional CT angiography of the thoracoabdominal aortic aneurysm alongside a hand-drawn schematic illustration used to guide fenestration planning. (B) Three-dimensional CT angiographic reconstruction illustrating the spatial orientation and directional alignment of the planned fenestrations relative to the visceral arteries. (C) Three-dimensional CT angiography demonstrating the angulation and curvature of the thoracoabdominal aorta, which is essential for accurate graft positioning and deployment planning. (D) Technical blueprint for fenestrated stent graft design based on anatomical measurements, and the finalized customized fenestrated stent graft fabricated accordingly. CT = computed tomography; Lt. = left; Rt. = right; SMA = superior mesenteric artery.



Figure 3. Fluoroscopic guidance and stent graft deployment during f-TEVAR. (A) Fluoroscopic image showing deployment of the customized fenestrated stent graft (SEAL 30-26×130 mm) into the thoracoabdominal aorta, with careful alignment of the fenestrations to the origins of the visceral arteries. (B) Fluoroscopic view of bridging stent graft placement into the right renal artery (BeGraft 6×38 mm) via the left brachial approach, followed by flaring ballooning using a Mustang 7×40 mm balloon. (C) Deployment of the bridging stent graft into the SMA (BeGraft 9×37 mm). (D) Bridging stent graft insertion into the left renal artery (Lifestream 7×37 mm) via the right femoral artery, with flaring ballooning performed using a Mustang 7×40 mm balloon. (E) Post-deployment fluoroscopic image demonstrating the in-situ fenestrated stent graft and all three bridging stent grafts accurately positioned. (F) Final digital subtraction angiography confirming preserved perfusion of the SMA and bilateral renal arteries without evidence of endoleak.

f-TEVAR = fenestrated thoracic endovascular aneurysm repair; SMA = superior mesenteric artery.

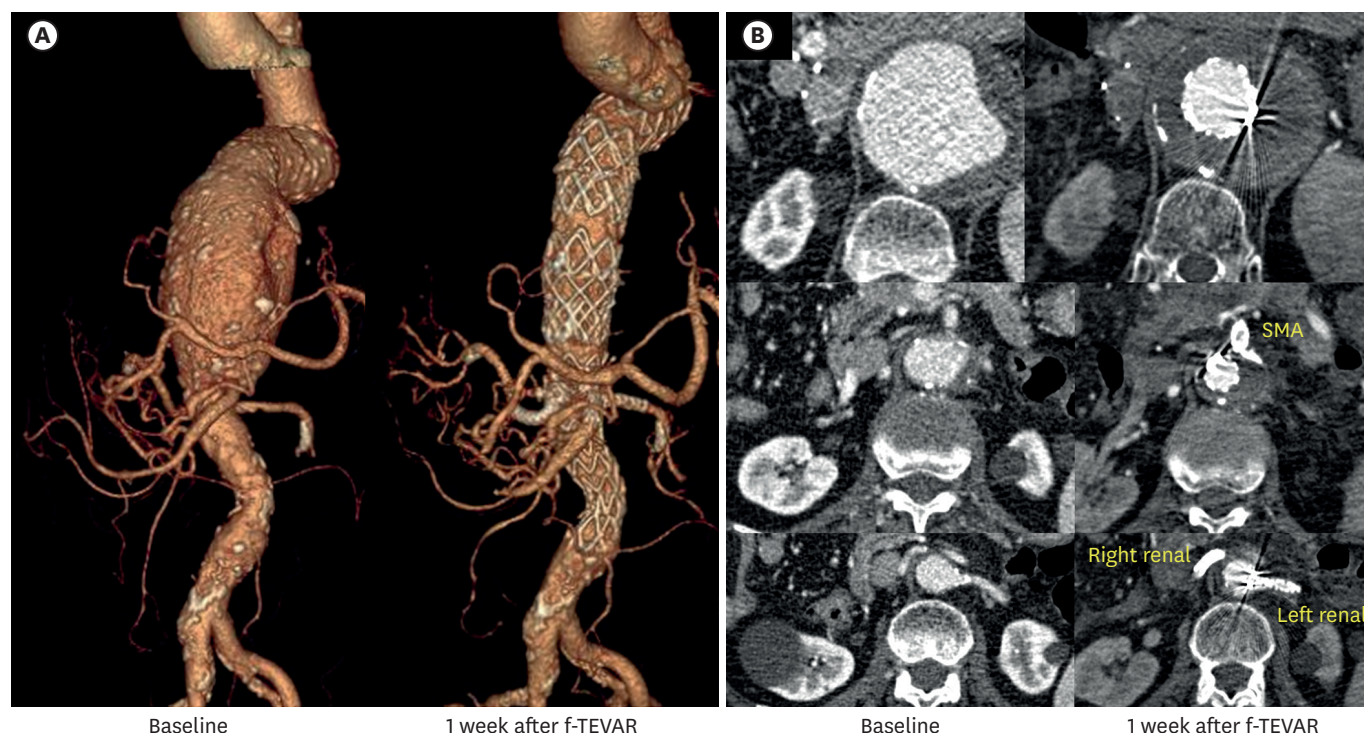


Figure 4. Comparison of pre- and post-procedural CT. (A) Volume-rendered 3-dimensional reconstructions before and after the procedure, demonstrating accurate alignment of the fenestrated stent graft to the visceral arteries. (B) Axial CT images demonstrating maintained patency of all bridging stent grafts to the SMA and both renal arteries, with no evidence of endoleak. CT = computed tomography; f-TEVAR = fenestrated thoracic endovascular aneurysm repair; SMA = superior mesenteric artery.

Conflict of Interest

The authors have no financial conflicts of interest.

Data Sharing Statement

The data generated in this study are available from the corresponding authors upon reasonable request.

Author Contributions

Conceptualization: Ko YG; Data curation: Jeong JC, Lee J, Kim SO; Formal analysis: Jeong JC, Ko YG; Supervision: Ko YG; Visualization: Jeong JC; Writing - original draft: Jeong JC; Writing - review & editing: Ko YG

REFERENCES

1. Wanhainen A, Van Herzele I, Bastos Goncalves F, et al. Editor's choice -- European Society for Vascular Surgery (ESVS) 2024 clinical practice guidelines on the management of abdominal aorto-iliac artery aneurysms. *Eur J Vasc Endovasc Surg* 2024;67:192-331. [PUBMED](#) | [CROSSREF](#)
2. Eagleton MJ, Follansbee M, Wolski K, Mastracci T, Kuramochi Y. Fenestrated and branched endovascular aneurysm repair outcomes for type II and III thoracoabdominal aortic aneurysms. *J Vasc Surg* 2016;63:930-42. [PUBMED](#) | [CROSSREF](#)
3. Elahwal M, Richards T, Imsirovic A, Bagga R, Almond G, Yusuf SW. Systematic review of the results of fenestrated endovascular aortic repair in octogenarians. *Ann R Coll Surg Engl* 2024;106:106-17. [PUBMED](#) | [CROSSREF](#)
4. Becker D, Fernandez Prendes C, Stana J, et al. Outcome of the be graft bridging stent in fenestrated endovascular aortic repair in a high-volume single center and an overview of current evidence. *J Endovasc Ther* 2024;15266028241231882. [PUBMED](#) | [CROSSREF](#)